

Erratum

Measurement of high- Q^2 charged-current e^+p deep inelastic scattering cross sections at HERA

The ZEUS Collaboration

Eur. Phys. J. C. **12**, 411–428 (2000) – DOI 10.1007/s100529900280

Published online: 21 December 1999 /

Erratum published online: 31 January 2003 – © Springer-Verlag / Società Italiana di Fisica 2003

With the aim of global fitting of parton distribution functions, the systematic uncertainties of this measurement have been broken down into uncorrelated sources and correlated sources. In the course of doing this, a mistake has been found in the procedure of adding up systematic uncertainties for the double-differential cross-section $d\sigma/dxdQ^2$, and has been fixed. This has altered the total systematic uncertainty of this quantity, with an insignificant effect on the total uncertainty. Corrected Table 4 and Figs. 7, 8 follow, as well as the details of uncorrelated and correlated systematic uncertainties for the cross-sections $d\sigma/dQ^2$, $d\sigma/dx$, $d\sigma/dy$ and $d\sigma/dxdQ^2$, shown in Tables 5 and 6.

Table 4. The double-differential cross-section $d\sigma/dxdQ^2$ for the reaction $e^+p \rightarrow \bar{\nu}_e X$. The following quantities are given for each bin: the x and Q^2 range; the values at which the cross section is quoted, x_c and Q_c^2 ; the number of selected events, N_{obs} ; the number of expected background events, N_{bg} ; the acceptance, \mathcal{A} ; the radiative correction factor, \mathcal{C}_{rad} (see Sect. 7); the measured Born-level cross section, $d\sigma/dxdQ^2$; and the Born-level cross section predicted by the Standard Model, using CTEQ4D PDFs. The first error of each measured cross-section value gives the statistical error, the second the systematic uncertainty

Q^2 range (GeV 2)	x range	Q_c^2 (GeV 2)	x_c	N_{obs}	N_{bg}	\mathcal{A}	\mathcal{C}_{rad}	$d^2\sigma/dxdQ^2(\text{pb}/\text{GeV}^2)$	
								measured	SM
200–400	0.0100–0.0215	280	0.015	50	2.0	0.64	1.00	$7.0^{+1.2}_{-1.0} \pm 0.7 \cdot 10^{-1}$	$5.27 \cdot 10^{-1}$
	0.0215–0.0464		0.032	42	4.7	0.80	0.99	$1.99^{+0.40}_{-0.34} {}^{+0.19}_{-0.18} \cdot 10^{-1}$	$2.07 \cdot 10^{-1}$
	0.0464–0.1000		0.068	28	5.9	0.71	0.97	$6.2^{+1.8}_{-1.5} \pm 1.0 \cdot 10^{-2}$	$7.49 \cdot 10^{-2}$
400–711	0.0100–0.0215	530	0.015	42	1.6	0.64	1.02	$3.86^{+0.72}_{-0.62} {}^{+0.33}_{-0.39} \cdot 10^{-1}$	$4.10 \cdot 10^{-1}$
	0.0215–0.0464		0.032	52	0.8	0.87	0.99	$1.62^{+0.26}_{-0.23} \pm 0.09 \cdot 10^{-1}$	$1.76 \cdot 10^{-1}$
	0.0464–0.1000		0.068	44	1.0	0.86	0.98	$6.4^{+1.1}_{-1.0} {}^{+0.3}_{-0.2} \cdot 10^{-2}$	$6.60 \cdot 10^{-2}$
	0.1000–0.1780		0.130	21	0.5	0.77	0.98	$2.41^{+0.67}_{-0.53} {}^{+0.13}_{-0.07} \cdot 10^{-2}$	$2.44 \cdot 10^{-2}$
711–1265	0.0100–0.0215	950	0.015	37	0.3	0.50	1.06	$2.97^{+0.58}_{-0.49} {}^{+0.30}_{-0.25} \cdot 10^{-1}$	$2.72 \cdot 10^{-1}$
	0.0215–0.0464		0.032	85	0.4	0.88	1.01	$1.53^{+0.19}_{-0.17} {}^{+0.04}_{-0.07} \cdot 10^{-1}$	$1.32 \cdot 10^{-1}$
	0.0464–0.1000		0.068	69	0.5	0.89	0.99	$5.59^{+0.76}_{-0.68} {}^{+0.12}_{-0.11} \cdot 10^{-2}$	$5.31 \cdot 10^{-2}$
	0.1000–0.1780		0.130	43	0.2	0.84	0.98	$2.61^{+0.46}_{-0.40} \pm 0.10 \cdot 10^{-2}$	$2.02 \cdot 10^{-2}$
	0.1780–0.3160		0.240	14	0.0	0.66	0.99	$5.7^{+2.0}_{-1.5} \pm 0.3 \cdot 10^{-3}$	$5.90 \cdot 10^{-3}$
1265–2249	0.0215–0.0464	1700	0.032	58	0.9	0.77	1.05	$6.9^{+1.1}_{-0.9} {}^{+0.3}_{-0.2} \cdot 10^{-2}$	$7.90 \cdot 10^{-2}$
	0.0464–0.1000		0.068	66	1.1	0.91	1.02	$3.03^{+0.43}_{-0.38} {}^{+0.05}_{-0.07} \cdot 10^{-2}$	$3.63 \cdot 10^{-2}$
	0.1000–0.1780		0.130	40	0.3	0.89	1.00	$1.31^{+0.24}_{-0.21} {}^{+0.01}_{-0.03} \cdot 10^{-2}$	$1.47 \cdot 10^{-2}$
	0.1780–0.3160		0.240	28	0.3	0.83	1.00	$5.1^{+1.2}_{-1.0} \pm 0.1 \cdot 10^{-3}$	$4.42 \cdot 10^{-3}$
2249–4000	0.0464–0.1000	3000	0.068	76	1.1	0.88	1.06	$2.12^{+0.28}_{-0.25} {}^{+0.02}_{-0.11} \cdot 10^{-2}$	$1.92 \cdot 10^{-2}$
	0.1000–0.1780		0.130	42	0.2	0.89	1.03	$8.0^{+1.4}_{-1.2} {}^{+0.2}_{-0.1} \cdot 10^{-3}$	$8.86 \cdot 10^{-3}$
	0.1780–0.3160		0.240	27	0.1	0.86	1.01	$2.79^{+0.65}_{-0.54} {}^{+0.08}_{-0.09} \cdot 10^{-3}$	$2.84 \cdot 10^{-3}$
	0.3160–0.5620		0.420	15	0.0	0.75	1.00	$9.5^{+3.2}_{-2.4} {}^{+0.4}_{-0.6} \cdot 10^{-4}$	$5.03 \cdot 10^{-4}$
4000–7113	0.0464–0.1000	5300	0.068	22	0.4	0.69	1.07	$6.3^{+1.7}_{-1.4} \pm 0.4 \cdot 10^{-3}$	$7.65 \cdot 10^{-3}$
	0.1000–0.1780		0.130	35	0.2	0.92	1.04	$3.75^{+0.75}_{-0.63} {}^{+0.23}_{-0.19} \cdot 10^{-3}$	$3.86 \cdot 10^{-3}$
	0.1780–0.3160		0.240	26	0.1	0.89	1.03	$1.51^{+0.36}_{-0.30} {}^{+0.07}_{-0.09} \cdot 10^{-3}$	$1.43 \cdot 10^{-3}$
	0.3160–0.5620		0.420	8	0.0	0.84	1.04	$2.7^{+1.3}_{-1.0} {}^{+0.3}_{-0.2} \cdot 10^{-4}$	$2.73 \cdot 10^{-4}$
7113–12649	0.1000–0.1780	9500	0.130	15	0.6	0.84	1.08	$1.06^{+0.37}_{-0.28} \pm 0.13 \cdot 10^{-3}$	$1.05 \cdot 10^{-3}$
	0.1780–0.3160		0.240	18	0.1	0.94	1.05	$5.6^{+1.7}_{-1.3} \pm 0.4 \cdot 10^{-4}$	$4.74 \cdot 10^{-4}$
	0.3160–0.5620		0.420	10	0.0	0.90	1.05	$1.82^{+0.78}_{-0.57} \pm 0.19 \cdot 10^{-4}$	$1.09 \cdot 10^{-4}$
12649–22494	0.1780–0.3160	17000	0.240	5	0.1	1.04	1.07	$8.0^{+5.5}_{-3.5} {}^{+1.7}_{-1.5} \cdot 10^{-5}$	$7.97 \cdot 10^{-5}$
	0.3160–0.5620		0.420	7	0.0	1.03	1.06	$6.3^{+3.4}_{-2.3} {}^{+1.0}_{-0.9} \cdot 10^{-5}$	$2.72 \cdot 10^{-5}$

Table 5. The differential cross-sections $d\sigma/dQ^2$, $d\sigma/dx$ and $d\sigma/dy$ for the reaction $e^+p \rightarrow \bar{\nu}_e X$. The following quantities are given for each bin: the value at which the cross section is quoted; the measured Born-level cross section; the statistical uncertainty; the total systematic uncertainty; the uncorrelated systematic uncertainty and those systematic uncertainties with significant (assumed 100%) correlations between cross-section bins. The systematic uncertainties considered to be correlated were: the FCAL energy scale (δ_1); the BCAL energy scale (δ_2) and the uncertainty in the parton-shower scheme (δ_3)

$d\sigma/dQ^2$							
Q_c^2	$d\sigma/dQ^2$ (pb/GeV 2)	δ_{stat} (%)	δ_{sys} (%)	δ_{unc} (%)	δ_1 (%)	δ_2 (%)	δ_3 (%)
280	$2.94 \cdot 10^{-2}$	± 9.5	$\pm 12.$	$+8.4$ -8.3	-1.0 $+2.4$	-1.0 $+1.9$	-7.9 $+7.9$
530	$1.82 \cdot 10^{-2}$	± 7.8	± 4.2 -4.5	$+3.6$ -3.7	-1.4 $+1.0$	-1.2 $+0.7$	-1.9 $+1.9$
950	$1.29 \cdot 10^{-2}$	± 6.4	± 2.3 -2.2	$+2.0$ -1.8	$+0.3$ $+0.5$	-1.0 $+1.0$	-0.5 $+0.5$
1700	$5.62 \cdot 10^{-3}$	± 7.1	± 1.5 -1.4	$+1.0$ -1.1	$+0.4$ -0.2	$+0.5$ $+0.0$	$+0.9$ -0.9
3000	$2.62 \cdot 10^{-3}$	± 7.8	± 1.3 -3.3	$+0.8$ -1.2	$+0.6$ -2.1	$+0.4$ -2.2	-0.8 $+0.8$
5300	$7.91 \cdot 10^{-4}$	$\pm 12.$ $-11.$	± 4.8 -3.9	$+0.8$ -0.6	$+3.0$ -1.7	$+3.6$ -3.4	$+0.4$ -0.4
9500	$2.00 \cdot 10^{-4}$	$\pm 18.$ $-15.$	± 8.6	± 0.7	$+4.4$ -4.5	$+7.1$ -7.0	$+2.2$ -2.2
17000	$2.61 \cdot 10^{-5}$	$\pm 37.$ $-28.$	$\pm 17.$ $-15.$	$+1.3$ -1.0	$+7.1$ -5.6	$+15.$ $-13.$	$+3.3$ -3.3
30000	$5.9 \cdot 10^{-7}$	$\pm 233.$ $-84.$	$\pm 30.$ $-26.$	$+3.2$ -3.3	$+9.0$ -9.4	$+28.$ $-23.$	$+7.6$ -7.6
$d\sigma/dx$							
x_c	$d\sigma/dx$ (pb)	δ_{stat} (%)	δ_{sys} (%)	δ_{unc} (%)	δ_1 (%)	δ_2 (%)	δ_3 (%)
0.015	$4.50 \cdot 10^2$	± 8.8	± 7.6 -7.9	± 6.1	-1.0 $+1.5$	-2.3 $+0.6$	-4.3 $+4.3$
0.032	$2.64 \cdot 10^2$	± 6.6	± 2.7 -2.6	± 2.4 -2.5	-0.2 $+0.2$	-0.3 $+0.7$	-0.7 $+0.7$
0.068	$1.44 \cdot 10^2$	± 5.9	± 1.9 -2.2	± 1.5	-0.4 $+0.5$	$+0.4$ -1.2	-1.0 $+1.0$
0.130	$6.88 \cdot 10^1$	± 7.2	± 2.4 -1.8	± 1.2	$+0.4$ -0.3	$+2.0$ -1.3	-0.1 $+0.1$
0.240	$2.57 \cdot 10^1$	± 9.0	± 3.5 -3.7	± 1.0	$+2.8$ -3.2	$+1.8$ -1.6	$+0.2$ -0.2
0.420	$6.8 \cdot 10^0$	$\pm 17.$ $-15.$	± 8.3 -8.4	± 2.4	$+7.8$ -7.9	$+0.9$ -1.1	$+1.5$ -1.5
0.650	$8.1 \cdot 10^{-1}$	$\pm 97.$ $-54.$	$\pm 26.$ $-20.$	$+5.2$ -5.1	$+25.$ $-19.$	$+2.1$ -0.9	$+1.3$ -1.3
$d\sigma/dy$							
y_c	$d\sigma/dy$ (pb)	δ_{stat} (%)	δ_{sys} (%)	δ_{unc} (%)	δ_1 (%)	δ_2 (%)	δ_3 (%)
0.05	$6.95 \cdot 10^1$	± 7.5	± 4.1	± 3.7	-0.8 $+0.9$	-0.5 $+0.1$	-1.3 $+1.3$
0.15	$5.92 \cdot 10^1$	± 6.5	± 2.4	± 1.2	$+0.3$ -0.5	-0.8 $+0.8$	-1.8 $+1.8$
0.27	$4.27 \cdot 10^1$	± 6.5	± 2.5 -2.2	± 1.9 -1.8	$+1.2$ -0.8	-0.5 $+0.9$	-0.9 $+0.9$
0.41	$3.52 \cdot 10^1$	± 7.6	± 2.2 -2.4	± 2.1 -2.2	$+0.5$ -0.2	$+0.3$ -0.6	-0.2 $+0.2$
0.55	$2.46 \cdot 10^1$	± 9.6	± 3.6 -3.2	± 2.8 -2.6	$+0.4$ $+0.2$	$+2.0$ -1.4	-1.1 $+1.1$
0.69	$1.55 \cdot 10^1$	$\pm 15.$ $-13.$	± 4.6 -6.7	± 3.2 -3.4	-0.9 -1.0	$+3.1$ -5.6	-1.0 $+1.0$
0.83	$1.49 \cdot 10^1$	$\pm 18.$ $-16.$	± 8.9 -8.8	± 5.6 -5.8	$+1.7$ $+0.5$	$+5.8$ -5.7	-3.4 $+3.4$

Table 6. The double differential cross-section $d\sigma/dxdQ^2$ for the reaction $e^+p \rightarrow \bar{\nu}_e X$. The following quantities are given for each bin: the Q^2 and x values at which the cross section is quoted, Q_c^2 and x_c ; the measured Born-level cross section; the statistical uncertainty; the total systematic uncertainty; the uncorrelated systematic uncertainty and those systematic uncertainties with significant (assumed 100%) correlations between cross-section bins. The systematic uncertainties considered to be correlated were: the FCAL energy scale (δ_1); the BCAL energy scale (δ_2) and the uncertainty in the parton-shower scheme (δ_3)

$Q_c^2(\text{GeV}^2)$	x_c	$d^2\sigma/dxdQ^2$ (pb/GeV 2)	δ_{stat} (%)	δ_{sys} (%)	δ_{unc} (%)	δ_1 (%)	δ_2 (%)	δ_3 (%)
280	0.015	$7.0 \cdot 10^{-1}$	+17. -15.	+9.2 -9.9	± 5.5	-1.8 +1.3	-3.6 +1.1	-7.2 +7.2
280	0.032	$1.99 \cdot 10^{-1}$	+20. -17.	+9.6 -9.1	+3.5 -3.9	-1.1 +2.3	+0.6 +3.0	-8.1 +8.1
280	0.068	$6.2 \cdot 10^{-2}$	+29. -24.	$\pm 17.$	$\pm 16.$	-1.4 +3.1	+0.3 -0.1	-5.0 +5.0
530	0.015	$3.86 \cdot 10^{-1}$	+19. -16.	+8.6 -10.	+7.9 -8.4	-2.3 +0.8	-3.2 -1.0	-3.4 +3.4
530	0.032	$1.62 \cdot 10^{-1}$	+16. -14.	± 5.4	± 5.0	-0.4 -1.0	-1.6 +1.9	-0.6 +0.6
530	0.068	$6.4 \cdot 10^{-2}$	+18. -15.	+4.5 -3.7	+1.9 -2.2	-1.9 +3.2	+0.5 +0.8	-2.3 +2.3
530	0.130	$2.41 \cdot 10^{-2}$	+28. -22.	+5.5 -3.1	+3.8 -2.3	-0.4 +2.9	+1.5 +0.5	+1.9 -1.9
950	0.015	$2.97 \cdot 10^{-1}$	+19. -17.	+10. -8.5	+8.8 -8.2	+1.7 +3.5	-1.6 +2.8	-1.4 +1.4
950	0.032	$1.53 \cdot 10^{-1}$	+12. -11.	+2.8 -4.4	+1.9 -2.0	-0.4 +0.0	-3.3 +0.4	+2.0 -2.0
950	0.068	$5.59 \cdot 10^{-2}$	+14. -12.	+2.2 -2.0	+1.6 -1.0	-0.1 -0.1	-1.0 +0.6	-1.4 +1.4
950	0.130	$2.61 \cdot 10^{-2}$	+18. -15.	+3.8 -3.6	+1.4 -1.3	+0.6 +0.2	-0.8 +1.2	-3.3 +3.3
950	0.240	$5.7 \cdot 10^{-3}$	+35. -27.	+5.4 -4.9	+3.2 -3.1	+1.3 +0.0	+1.5 +0.4	-3.9 +3.9
1700	0.032	$6.9 \cdot 10^{-2}$	+15. -13.	+4.3 -3.1	+3.2 -2.6	-0.1 +0.8	+2.1 +0.9	+1.8 -1.8
1700	0.068	$3.03 \cdot 10^{-2}$	+14. -13.	+1.6 -2.2	+0.5 -0.8	+0.6 +0.2	-1.6 +0.0	+1.4 -1.4
1700	0.130	$1.31 \cdot 10^{-2}$	+19. -16.	+1.1 -1.9	+0.8 -1.5	-0.2 -0.7	+0.8 -1.0	+0.2 -0.2
1700	0.240	$5.1 \cdot 10^{-3}$	+23. -19.	+2.6 -1.9	+1.1 -0.7	+2.1 -1.7	+1.1 -0.1	+0.5 -0.5
3000	0.068	$2.12 \cdot 10^{-2}$	+13. -12.	+1.1 -5.1	+0.6 -1.9	-1.3 -1.9	+0.5 -4.1	-0.8 +0.8
3000	0.130	$8.0 \cdot 10^{-3}$	+18. -15.	+1.9 -1.6	+0.6 -0.5	+1.1 -1.3	+0.7 +1.0	-0.8 +0.8
3000	0.240	$2.79 \cdot 10^{-3}$	+23. -19.	+2.8 -3.2	+0.9 -0.8	+2.5 -2.9	-0.8 +0.6	+0.3 -0.3
3000	0.420	$9.5 \cdot 10^{-4}$	+33. -26.	+4.5 -6.3	+0.9 -1.4	+3.9 -5.7	+0.4 -0.9	-2.1 +2.1
5300	0.068	$6.3 \cdot 10^{-3}$	+27. -22.	+5.5 -5.8	+1.6 -1.3	+1.5 +2.2	+4.3 -5.4	-1.5 +1.5
5300	0.130	$3.75 \cdot 10^{-3}$	+20. -17.	+6.1 -5.1	+1.3 -0.4	+1.3 -0.8	+5.2 -4.4	+2.5 -2.5
5300	0.240	$1.51 \cdot 10^{-3}$	+24. -20.	+4.9 -5.8	+0.6 -0.7	+4.8 -5.7	+0.8 -1.1	-0.3 +0.3
5300	0.420	$2.7 \cdot 10^{-4}$	+49. -35.	+9.8 -7.6	+1.3 -0.5	+9.6 -7.6	+0.6 +0.9	+0.0 +0.0
9500	0.130	$1.06 \cdot 10^{-3}$	+35. -27.	$\pm 12.$	+1.4 -1.5	+0.7 -1.3	+12. -11.	+3.8 -3.8
9500	0.240	$5.6 \cdot 10^{-4}$	+30. -23.	+6.4 -7.7	± 0.7	+4.9 -5.4	+3.7 -5.2	+1.6 -1.6
9500	0.420	$1.82 \cdot 10^{-4}$	+43. -31.	$\pm 11.$	+0.5 -0.6	$\pm 11.$	-0.3 -0.2	-0.5 +0.5
17000	0.240	$8.0 \cdot 10^{-5}$	+69. -44.	+21. -19.	+1.8 -1.7	+1.0 -1.2	+20. -19.	+3.5 -3.5
17000	0.420	$6.3 \cdot 10^{-5}$	+54. -37.	+16. -14.	± 0.9	+14. -13.	+4.6 -3.3	+3.5 -3.5

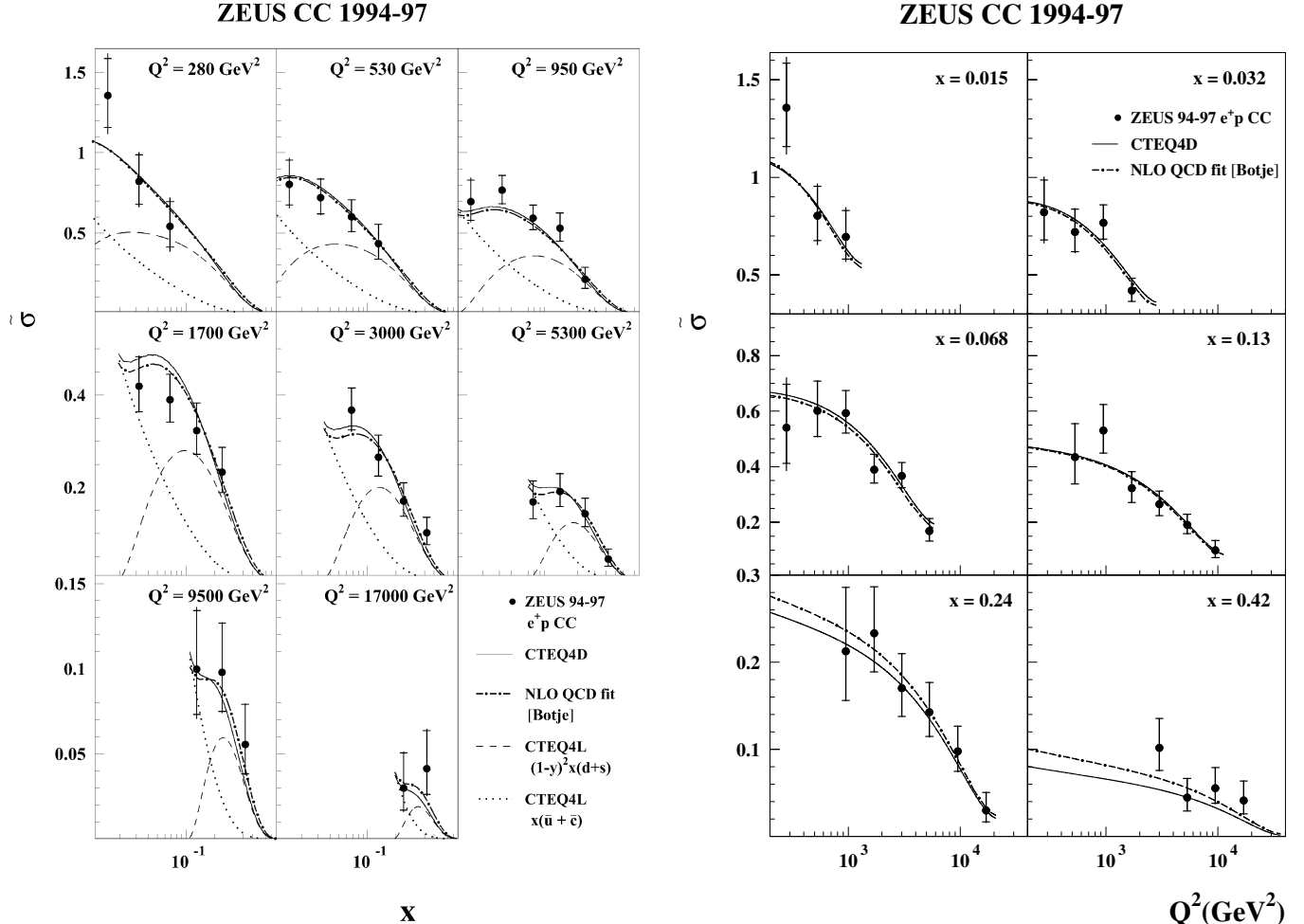


Fig. 7. The reduced cross-section $\tilde{\sigma}$ as a function of x , for fixed values of Q^2 . The dots represent the data, while the expectations of the Standard Model evaluated using the CTEQ4D PDFs are shown as the solid lines. For illustration, the leading-order PDF combinations $x(\bar{u} + \bar{c})$ and $(1 - y)^2 x(d + s)$, taken from the CTEQ4L parameterization, are plotted as dotted and dashed lines, respectively. Also shown is the result of the NLO QCD fit (*dash-dotted line*)

Fig. 8. The reduced cross-section $\tilde{\sigma}$ as a function of Q^2 , for fixed values of x . The dots represent the data, while the expectations of the Standard Model evaluated using the CTEQ4D PDFs are shown as the solid lines. Also shown is the result of the NLO QCD fit (*dash-dotted line*)